J Fluoresc (2013) 23:591–597
DOI 10.1007/s10895-013-1208-8

ORIGINAL PAPER

Prism-based Spectral Imaging of Four Species of Single-molecule Fluorophores by Using One Excitation Laser

Takanobu Haga · Tsuyoshi Sonehara · Takeshi Fujita · Satoshi Takahashi

Received: 6 February 2013 / Accepted: 24 February 2013 / Published online: 8 March 2013

Abstract A prism-based imaging system for simultaneously detecting four species of single-molecule (SM) fluorophores was developed. As for the detection method, four spectrally distinct species of BigDye fluorophores were bound to 50-nm-diameter gold nanoparticles (AuNPs) to form AuNP/BigDye complexes. Four species of complexes were randomly immobilized on different fused-silica slides. BigDyes were excited by an argon-ion-laser (excitation wavelengths: 488 and 514.5 nm) beam through total internal reflection on the slide surface. SM fluorescence emitted from a complex was spectrally dispersed through a prism to form an SM spot elongated in the spectral direction on a charge-coupled device. A scattered light spot generated by the AuNP of the same complex under 594-nm laser illumination was used as a wavelength reference, and the SM fluorescence spectrum was obtained from the pixel-intensity pattern of the elongated SM spot. Peak locations of fluorescence spectra of all the observed SM spots were obtained, and their histograms were distinctly separated according to species. SM spots can thus be classified as one of four species according to their peak locations. By statistically analyzing the histograms, the classification accuracy was estimated to be above 93.8 %. The number of pixels in the spectral direction required for classifying four species of SM fluorophores was estimated to be 10. As for the conventional system (which uses two excitation lasers), 15 pixels are required. Using BigDyes as the four fluorophores (which consist of donors linked to acceptors and can be excited by just an argon-ion laser) is the reason that such a small number of pixels was achieved. The developed system can thus detect 1.5 times more SM fluorophores per field of view; that is, its throughput is 1.5 times higher. The approach taken in this study, namely, using BigDye with a prism-type system, is effective for increasing the throughput of DNA microarray-chip analysis and SM real-time DNA sequencing.

Keywords Prism · Spectral imaging · Four colors · Single molecule · BigDye · Fluorescence-resonance energy transfer

T. Haga (✉) · T. Sonehara · T. Fujita
Central Research Laboratory, Hitachi, Ltd.,
1-280 Higashi-Koigakubo,
Kokubunji-shi, Tokyo 185-8601, Japan
e-mail: takanobu.haga.uw@hitachi.com

S. Takahashi
Research and Development Division,
Hitachi High-Technologies Corporation, 882 Ichige,
Hitachinaka-shi, Ibaraki-ken 312-8504, Japan

Introduction

Spectral-imaging systems for detecting multi-colors of single-molecule (SM) fluorophores are widely used for biological studies [1–6], DNA microarray-chip analysis [7], and real-time DNA sequencing [8, 9]. Although many types of systems are conventionally available (i.e., filter-wheel [10], dichroic-mirror [1–7, 11–13], Fourier-transform [14], and prism [15–18]), the dichroic-mirror type and prism type are mainly used for such studies. Since these two types require no mechanical movement for resolving multi-colors of a spectrum, they can achieve both high temporal resolution and high sensitivity.

The dichroic-mirror-type system classifies multi-species of fluorophores by resolving each species of fluorescence signals with dichroic mirrors and detecting them with a dedicated image sensor. The configuration of this type of system, however, becomes complex and expensive as the number of fluorescence species increases. This problem becomes pronounced when the number of fluorescence

species is above three and when expensive image sensors such as cooled charge-couple devices (CCDs) are used for achieving high SM sensitivity [11]. A "quad-view" system can simultaneously image four species of fluorophores with only one image sensor [13]. The throughput (i.e., number of SM fluorophores detectable in the field of view) of the system, however, is one-fourth that of an imaging system with four image sensors [11].

In contrast, the prism-type system uses one image sensor regardless of the number of fluorescence species, so its configuration is simple and less expensive. Eid et al. have developed a prism-type imaging system (called a conventional prism-type system, hereafter) for "SM real-time DNA sequencing" [8, 15]. In this system, two laser beams are introduced into a slide, on which four species of SM fluorophores are immobilized on a grid. Fluorescence from an SM fluorophore is collected with an objective lens and dispersed through a prism to give an SM fluorescence spot (SM spot) that is a pixel-intensity pattern elongated on the image sensor in the spectral direction. The pixel-intensity pattern represents a fluorescence spectrum, so the SM fluorophore can be classified as one of four fluorophore species. The conventional prism-type system, however, has two problems (as explained in the following two paragraphs).

In a prism-type system, a pixel-intensity pattern of an SM spot cannot represent a fluorescence spectrum unless a wavelength axis is provided. Two approaches can be used for providing this wavelength axis. The first approach is to use a wavelength reference, which should be a point source with a known emission spectrum at the same position as the SM fluorophore. Sonehara et al. have imaged SM fluorophores bound to 50-nm-diameter gold nanoparticles (AuNPs) with a prism-type system [16]. In their system, an AuNP photoluminescence spot is used as a wavelength reference for each SM spot, so the fluorescence spectrum is obtained from the pixel-intensity pattern. Accordingly, the system distinguishes two species of SM fluorophores spaced randomly on fused-silica slides. Moreover, the preparation of the slides is simple, namely, mixing solutions to form AuNP/fluorophore complexes and infusing them onto the slides for immobilization [16]. The above-mentioned conventional prism-type system uses the second approach, namely, spacing SM fluorophores on a grid. The positions of grid-spaced SM fluorophores are known, so the wavelength axes are already provided; however, the preparation of the slide requires complex semiconductor processing [19].

The pixel area of the image sensor occupied by one SM fluorophore ("SM area", hereafter) in the conventional prism-type system is large, namely, 75 pixels (i.e., 15 pixel (spectral direction) × 5 pixels (non-spectral)) [15]. The SM area includes the pixel areas corresponding to the excitation-wavelength regions. The conventional prim-type system excites four species of fluorophores simultaneously with 532-nm and 643-nm lasers [8]. The 643-nm excitation light between two fluorescence spectra is removed with a notch filter, so the pixel area corresponding to the removed-wavelength region is not used for fluorescence detection. Although 532-nm excitation light is also removed, the corresponding pixel area can be used as a part of an adjacent SM area. Under the assumption that the bandwidth of the notch filter for 643-nm excitation light is above 30 nm, the unused pixel area per SM area is above 10 pixels. (Reciprocal linear dispersion is 15 nm/pixel, so the unused pixel area is calculated as 30 nm/15 nm/pixel (spectral direction) × 5 pixels (non-spectral) [15].) Removing the unused pixel area thus increases the throughput of the conventional prism-type system by more than 13 % (i.e., 10 pixels/75 pixels × 100 %).

In this work, a prism-type system for simultaneously detecting four species of randomly-spaced SM fluorophores—with higher throughput than the conventional prism-type system—is proposed. SM fluorophores are bound to AuNPs and scattered light of AuNP is used as a wavelength reference, so the system can detect randomly-spaced SM fluorophores. BigDye® fluorophores (Life Technologies, Carlsbad, CA) were used as four species of fluorophores. The structure of BigDye consists of a donor linked to an acceptor. BigDye uses fluorescence-resonance energy transfer to emit fluorescence of an acceptor. The donor used is fluorescein, and four species of dichloro-rhodamine acceptors are used [20]: dichloro-rhodamine 6G (dR6G), dichloro-rhodamine 110 (dR110), dichloro-carboxytetramethyl-rhodamine (dTAMRA), and dichloro-carboxy-X-rhodamine (dROX). Hereafter, the four DigDyes are distinguished by their acceptors (dR6G, dR110, dTAMRA, and dROX). The excitation maximum of the four species of BigDyes is that of the fluorescein donor, so all four species can be excited by the same excitation laser as that for exciting fluorescein, namely, an argon-ion laser (excitation wavelengths: 488 and 514.5 nm). The proposed prism-type system thus has no unused pixel area and can achieve higher throughput. Four species of BigDye were bound to AuNPs, and AuNP/BigDye complexes were randomly immobilized on fused-silica slides. Each of the four species of these complexes on the slide was irradiated by the argon-ion laser through total internal reflection (TIR) on the slide surface. SM fluorescence and photoluminescence emitted from an AuNP/BigDye complex were detected by the prism-type system. With scattered light of AuNP under illumination of 594-nm HeNe laser used as a wavelength reference, the fluorescence spectrum of each SM BigDye was obtained from a pixel-intensity pattern of an SM spot. The classification accuracies of the four species were statistically estimated in accordance with the peak locations of all the observed SM fluorescence spectra. Moreover, the

throughput relative to the conventional prism-type system was estimated in accordance with SM area.

Experimental

Preparation of BigDye-Immobilized Slides

A BigDye-immobilized slide is schematically illustrated in Fig. 1. An SM BigDye is bound to an AuNP by using thiolated double-stranded (ds) DNA as a linker, where a thiol group (−SH) specifically links to the AuNP. A complex of BigDye and an AuNP is immobilized on a cetyltrimethylammonium bromide (CTAB)-coated surface of the fused-silica slide. In regard to this configuration, thiolated dsDNA is chosen as a linker between the BigDye and AuNP because BigDye is commercially available as "BigDye primer", namely, a single-stranded (ss) DNA with BigDye labeled at its 5′ end. On the other hand, an ssDNA that has a sequence complementary to the BigDye primer and thiol group at its 5′ end (complementary ssDNA) is also commercially available. Hybridizing the complementary ssDNA with BigDye primer can thus provide the linker to BigDye.

Four species of BigDye Primer were purchased as "BigDye Primer mix" solutions (ABI PRISM® BigDye® Primer Cycle Sequencing Ready Reaction Kit, Life Technologies, Carlsbad, CA). Each of the four solutions contains one species of BigDye primers. The primer sequence is 5′-BigDye-TGT AAA ACG ACG GCC AGT-3′. The BigDye primer was hybridized with the complementary ssDNA (Sigma Genosys, Japan) as described below. The 32-mer sequence of the complementary ssDNA is 5′-SH-TT TTT TTT TTT TTT ACT GGC CGT CGT TTT ACA-3′. In the hybridization process, 1.4 μL of 5.4-μM complementary ssDNA solution was first mixed with 23 μL of ca.350-nM "BigDye Primer mix" solution and then annealed with a thermal cycler. The temperature of the thermal cycler was decreased from 95 to 60 °C in five-degree increments, kept constant for 2.5 min after each incremental decrease, and, finally, kept at 55 °C for 5 min. The hybridization process was repeated for all four BigDye species to prepare four BigDye-labeled dsDNA solutions.

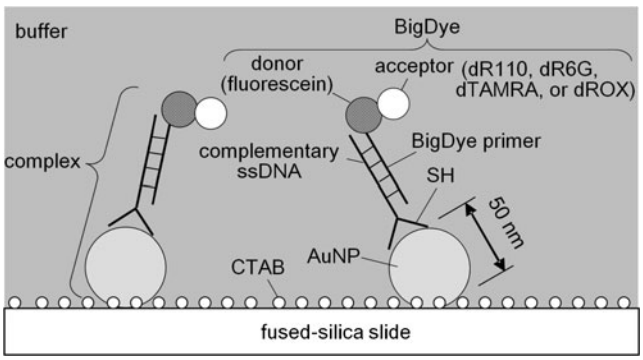

Fig. 1 Schematic illustration of BigDye-immobilized slides. Gold nanoparticle (AuNP)/BigDye complexes are immobilized in TM buffer on a fused-silica slide coated with cetyltrimethylammonium bromide (CTAB). BigDye primer labeled with BigDye is hybridized with complementary ssDNA modified with thiols and binds to 50-nm AuNP through a thiol group (−SH). "BigDye" is one of four species: dR110, dR6G, dTAMRA, or dROX

15 μL of the BigDye-labeled dsDNA solution, 10 μL of 9-nM AuNP solution, 8 μL of 100-mg/mL Bis (p-sulfonatophenyl) phenylphosphine dihydrate dipotassium salt (BSPP, STREM CHEMICALS, Newburyport, MA), and 57 μL of purified water (with resistance greater than 17.6 MΩ) were mixed and shaken to form thiol-AuNP linkage. The mixed solution was then purified and unreacted BigDye-labeled dsDNAs were removed. Accordingly, a solution of 1-nM AuNP/BigDye complex was obtained. The detailed mixing and purification processes are described in Ref. [16]. The process above was repeated for all four BigDye species.

The immobilization process was performed in a flow cell consisting of a fused-silica slide (50×26×0.9 mm, Hikari Kobo, Japan), a coverslip (18×18 mm, Matsunami Glass, Japan), and two sheets of 25-μm-thick spacers (Lumirror 25-S10, Toray, Japan). First, two solutions were successively infused into the flow cell: 10 μL of 0.8-mM CTAB solution and 10 μL of 1-nM AuNP/BigDye complex solution. After each infusion, the flow cell was incubated for 3 min and washed with 100 μL of TM buffer (10-mM tris–HCl; pH 7.8; 2-mM $MgCl_2$). Finally, the two spacer sheets were removed, and the flow cell was sealed with a top-coat manicure (*Keshowakusei*, Shiseido Company, Japan). Four BigDye-immobilized slides (dR6G, dR110, dTAMRA, and dROX slide) were thus prepared in this manner.

Spectral Imaging

A block diagram of the developed prism-type imaging system is shown in Fig. 2. In the first step of the imaging process, the shutter for the argon-ion laser is opened, and

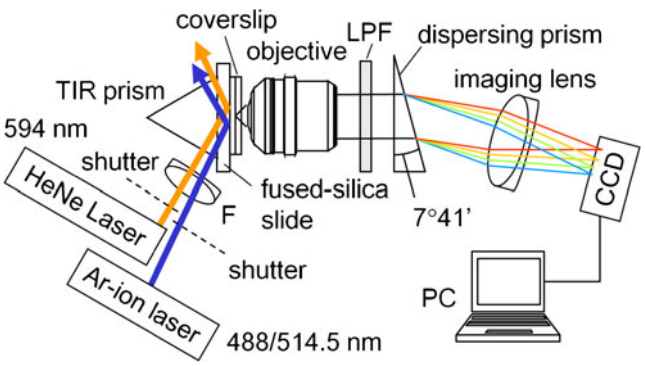

Fig. 2 Block diagram of prism-type imaging system. *TIR*, total internal reflection; *F*, focusing lens; *LPF*, long-pass filter; *PC*, personal computer

that for the He-Ne laser is closed. The beam from a continuous-wave argon-ion laser oscillating at 488 and 514.5 nm simultaneously (2214-40MLA, Uniphase, USA) passes through a focusing lens, a TIR prism, and onto either the dR6G, dR110, dTAMRA, or dROX slide. Entering the slide through a glycerol layer between the TIR prism and the slide, the beam is totally reflected at a reflection angle of 69° on the BigDye-immobilized surface of the slide and generates an evanescent field. The total power and $1/e^2$ diameter of the beam just before the TIR are 30 mW and 0.2 mm, respectively. Each AuNP/BigDye complex is excited by the evanescent field and emits fluorescence, AuNP photoluminescence, and scattered light. These emissions are collected by a water-immersion objective lens with a numerical aperture of 1.2 and focal length of 3 mm (UPLSAPO 60× W, Olympus, Japan), and the scattered light is rejected by a long-pass filter, LPF (LP02-514RU-25, Semrock, Rochester, NY). Passing through a dispersing prism made of BK7 with a wedge angle of 7°41′ (45559-I, Edmund Optics, Barrington, NJ) and an imaging lens with a focal length of 85 mm (47640-I, Edmund Optics, Barrington, NJ), the fluorescence and AuNP photoluminescence form fluorescence spots and photoluminescence spots, respectively, on a CCD with 1,392×1,040 pixels, where the size of each pixel is 6.45× 6.45 μm (C4752-12-AG, Hamamatsu, Japan). The dispersing prism is set so that spectra are dispersed along the longer side of the CCD imaging area. Immediately after the shutter for the argon-ion laser was opened, the CCD operating in continuous-shoot mode generates 12-bit digital images for 24 s at a frame interval of 0.12 s, and these images are uploaded to the hard disc of a personal computer through an IEEE1394 interface. In this manner, a series of images (signal images) is acquired

In the second step, the shutter for the argon-ion laser is closed, and that for the 594-nm He-Ne laser is opened. The beam of the He-Ne laser follows the same path as that of the argon-ion laser. Under the illumination of the He-Ne laser, each AuNP/BigDye complex emits strong 594-nm scattered light, which forms a scattered-light spot on the CCD. The scattered-light spot is used as a wavelength reference. A series of images (reference images) is similarly acquired with the CCD for 2.4 s at a frame interval of 0.12 s.

Results and Discussion

Image Analysis of BigDye-Immobilized Slides

A signal image and reference image of the dROX slide are shown in Fig. 3(a) and (b), respectively. Arrows 1, 2, and 3 indicate the photoluminescence spot, fluorescence spot, and scattered light spot of the same AuNP/dROX complex, respectively. The two spots largely elongated in the spectral direction in Fig. 3(a) did not photobleach over time.

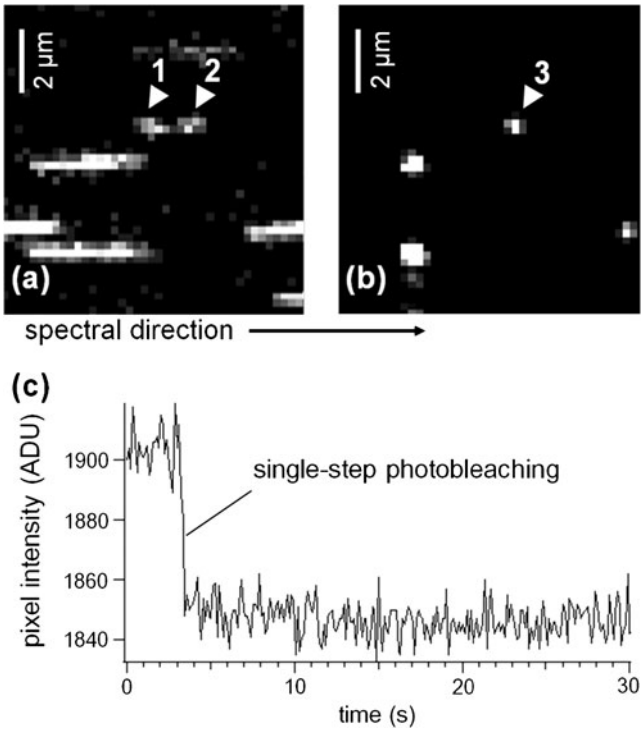

Fig. 3 **a** Signal image and **b** reference image for dROX slide. *Arrows 1, 2, and 3* indicate a photoluminescence spot, a fluorescence spot, and a scattered light spot of the same AuNP/dROX complex, respectively. **c** Waveform of pixel intensity of a dROX fluorescence spot (*arrow 2*) as a function of time. Waveform exhibited single-step photobleaching indicating that spot originated from single-molecule (SM) dROX

Moreover, it has been reported that aggregation can broaden photoluminescence at longer wavelengths, thereby elongating spots in the spectral direction [21, 22]. It is thus concluded that the two spots are probably photoluminescence spots of aggregated AuNPs. The waveform of pixel intensity of the fluorescence spot indicated by arrow 2 is shown in Fig. 3(c) as a function of time. The waveform exhibited a single-step photobleaching [23], indicating that the spot originated from SM dROX. Similar single-step photobleachings were observed for the other three species of fluorescence spots (dR110, dR6G, and dTAMRA). Such spots were regarded as SM spots. It is therefore concluded from these results that fluorescence of SM BigDyes was successfully detected.

A pixel-intensity pattern of an SM spot in the spectral direction represents a fluorescence spectrum. Only SM spots from signal images were picked out, and the peak locations of their pixel-intensity patterns were determined with subpixel precision [16]. The peak locations are defined as the peak coordinates of their pixel-intensity patterns in a signal image relative to those of scattered light spots in a reference image. Peak locations of all the SM spots were obtained by following the image-analysis procedure described in Ref. [16]. Histograms of the peak locations of the four species of BigDyes are shown in Fig. 4. The histograms of

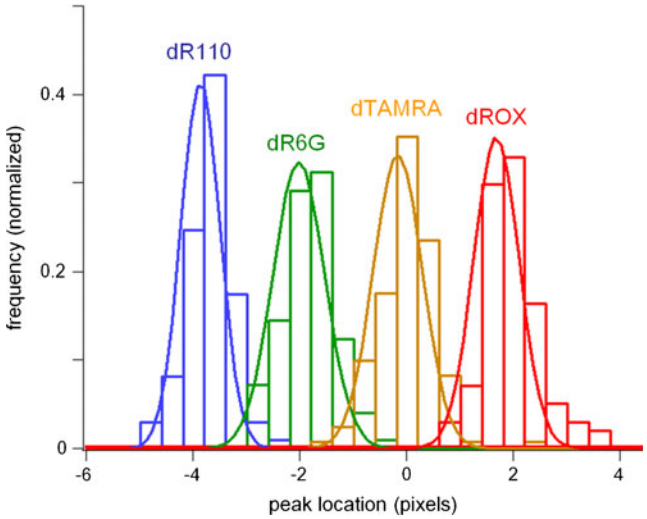

Fig. 4 Histograms of peak locations of four species of BigDyes. Numbers of SM spots are 97 for dR110, 96 for dR6G, 119 for dTAMRA, and 81 for dROX. Each histogram area is normalized. Histograms are fitted with a Gaussian function (*solid curves*)

dR110, dR6G, dTAMRA, and dROX consist of 97, 96, 119, and 81 SM spots, respectively. Each histogram area is normalized. The four histograms are distinctly separated with the same order as the fluorescence spectra of four species (i.e., dR110, dR6G, dTAMRA, and dROX) [20]. SM spots can thus be classified as one of four species in accordance with their peak locations.

Under the assumption that peak locations differ according to Gaussian profile, the histograms were fitted with a Gaussian function to obtain the means and standard deviations (solid curves in Fig. 4). The statistical results concerning the peak locations of the four BigDyes are listed in Table 1. The calculated relation between wavelength and peak location is plotted in Fig. 5.[1] The curve was plotted such that 594 nm corresponds to the peak location at zero pixels because the observed peak locations are the locations relative to 594-nm scattered light spots. The theoretically calculated means in Table 1 are the peak locations corresponding to the maximum of the fluorescence spectra of R110, dR6G, dTAMRA, and dROX (540, 566, 593, and 618 nm, respectively [20]) in Fig. 5. The means of the observed peak locations of four species agree well with the theoretically calculated means (Table 1). The value of dR110 (−3.94 pixels) is slightly larger than the theoretically calculated mean (−4.51 pixels). This discrepancy is caused

[1] The relation in Fig. 5 was calculated from the wedge angle of the dispersion prism (7°41′), the refractive index of the dispersion prism (BK7), the optical magnification (×28.3), and the pixel size of the CCD (6.45×6.45 μm^2/pixel). The refractive index (n) of BK7 at wavelength λ (unit: μm) is calculated by using the Sellmeier equation: $n = \{1 + 1.04\lambda^2 / (\lambda^2 - 0.006) + 0.232\lambda^2 / (\lambda^2 - 0.02) + 1.01\lambda^2 / (\lambda^2 - 104)\}^{1/2}$.

Table 1 Statistical results concerning peak locations (units in pixels)

Fluorophore (# of SM spots)	dR110 (97)	dR6G (96)	dTAMRA (119)	dROX (81)
Mean	−3.94	−2.11	−0.24	1.60
Standard deviation	0.46	0.47	0.51	0.49
Theoretically calculated mean	−4.51	−2.19	−0.07	1.66

by cutting off the fluorescence of less than 520 nm with the LPF (Fig. 2). Accordingly, the effective fluorescence spectrum of dR110 became asymmetric with a large tale on the long-wavelength side. Smoothing such an asymmetric spectrum by a 3×3-pixel scalar in the image analysis [16] shifted the observed peak to longer wavelength. The standard deviations of the peak locations are not sufficiently small (0.46–0.51 pixels) in comparison with the spacing between the histograms (1.83–1.87 pixels), so the histograms significantly overlap each other. SM spots in the overlapped area can be misclassified. The classification accuracy was thus estimated as described below.

Estimation of Classification Accuracy for BigDye

For classifying SM spots, three thresholds on peak-location value were set within the three overlapped areas between the histograms (Fig. 4). The peak-location axis is thus divided into four regions, each of which corresponds to one of the four species. An SM spot can be classified as the species whose region includes its peak location. For example, if a dR110 SM spot has a peak location within the dR6G region, the SM spot is incorrectly classified as dR6G. The rate for incorrectly classifying dR110 as dR6G is thus estimated as

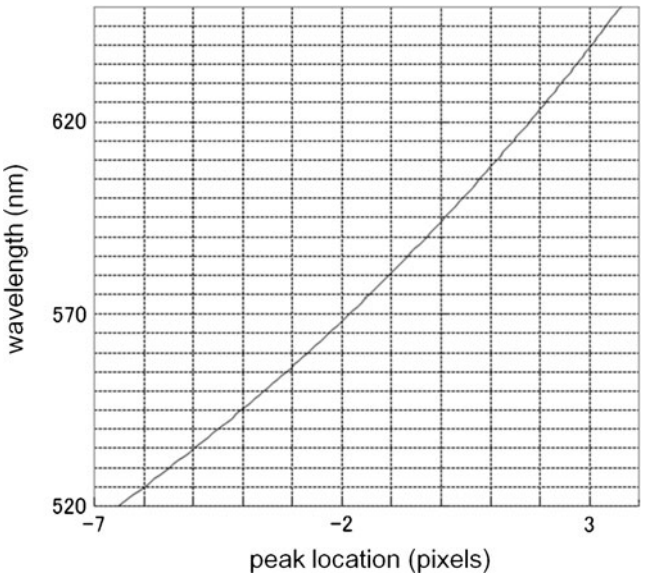

Fig. 5 Calculated relation between peak location and wavelength. Calculation method is described in[1]

Table 2 Estimated classification rates. The four values in bold text are correct classification rates; the others are incorrect classification rates

Classified result Fluorophore	dR110	dR6G	dTAMRA	dROX
dR110	**97.5 %**	2.5 %	0 %	0 %
dR6G	2.5 %	**94.7 %**	2.8 %	0 %
dTAMRA	0 %	2.8 %	**93.8 %**	3.4 %
dROX	0 %	0 %	3.4 %	**96.6 %**

the ratio of the number of dR110 SM spots with their peak locations within the dR6G region to the total number of dR110 SM spots. Under the assumption that the total number corresponds to the total area under the Gaussian curve, the rate is calculated as the ratio of the area of the dR6G region under the Gaussian curve of dR110 to the total area [16]. A threshold was set such that the rate for incorrectly classifying dR110 as dR6G and the rate for incorrectly classifying dR6G as dR110 are the same. The threshold is determined from the means and standard deviations of the two species [16]. Three thresholds were set, and the incorrect classification rates for all four species were acquired. A correct classification rate for a species is estimated by subtracting the sum of incorrect classification rates from one.

The estimated classification rates for the four species of BigDye are listed in Table 2. The rates are given as a percentage. The four values in bold indicate the correct classification rates; the others indicate the incorrect classification rates. The fact that two incorrect classification rates for the same combinations of species show the same values reflects the above-mentioned threshold setting. For example, the two rates for incorrectly classifying dR6G as dR110 and dR110 as dR6G are both 2.5 %. The classification rates for dR6G and dTAMRA (94.7 % and 93.8) are lower than those for dR110 and dROX (97.5 % and 96.6 %) because their histograms have two large overlapped areas between adjacent histograms; the others have only one overlapped area. The classification accuracy of the developed system was thus taken as the lowest rate, namely, 93.8 %. This value is lower than that of the conventional prim-type system (96 %).[2]

Increasing the spacing between the histograms and/or decreasing the standard deviations of peak locations will improve the accuracy. However, increasing the spacing further elongates the SM spots, thereby decreasing the throughput. It is thus necessary to decrease the standard deviations. Although the cause of the large standard deviations is not clear, it is probably attributable to monochromatic aberrations of the developed system. Among the monochromatic aberrations, coma, astigmatism, and distortion can significantly change pixel-intensity patterns of SM spots and scattered-light spots, so their peak locations can vary. On the other hand, the effect of chromatic aberrations was negligible. The more spectrally distinct a fluorophore species is from 594-nm scattered light of AuNPs, the more largely chromatic aberrations should vary peak locations. Accordingly, the standard deviation of the peak locations of dR110 would be the largest and that of the peak locations of dTAMRA would be the smallest. However, there is no such evidence in the observed values: 0.46 for dR110 and 0.51 for dTAMRA (Table 1). This finding is reasonable because the imaging lens (47640-I, Edmund Optics, Barrington, NJ) and objective lens (UPLSAPO 60× W, Olympus, Japan) of the developed system are achromatized over the wavelength region of fluorescence and 594-nm scattered light (i.e., 520–650 nm). As future work, the influence of the monochromatic aberrations on the standard deviations of peak locations will be evaluated. Eliminating these aberrations will improve the classification accuracy of the developed system above 96 %.

Throughput Estimation

The throughput of the developed system relative to that of the conventional prism-type system was estimated in accordance with SM area. The fluorescence spectra of the four species of BigDyes spread over a wavelength region of 520–650 nm [20], corresponding to ca. 9.5 pixels (Fig. 5). The developed system thus needs 10 pixels in the spectral direction for classifying the four species of BigDyes. The SM-spot size in the non-spectral direction is equivalent to the diffraction-limited diameter (<3 pixels), so spacing five pixels in the non-spectral direction is sufficient to prevent crosstalk between SM spots. The SM area of the developed system is thus 50 pixels (i.e., 5×10 pixels), whereas that of the conventional prism-type system is 75 pixels [15]. If the same CCD is used, the developed system can therefore detect 1.5 times (i.e., 75 pixels/50 pixels) more SM spots than the conventional prism-type system, thereby achieving 1.5-times-higher throughput.

Concluding Remarks

A prism-type imaging system for simultaneously detecting four species of SM BigDyes was developed and evaluated. AuNP/BigDye complexes were imaged to provide SM BigDye spots elongated in the spectral direction. The elongated SM spots represented fluorescence spectra, and their peak locations relative to scattered light spots generated by

[2] In reference [8], the DNA-sequencing result shows that seven out of 158 bases (i.e., 4 %) were identified as mismatch errors, which were mainly caused by fluorophore misclassifications. The classification accuracy of the conventional prism-type system is thus thought to be about 96 %.

AuNPs were determined. It was found that peak locations for the four species distinctly differ, so SM spots can be classified as one of four species in accordance with their peak locations. By statistically evaluating the histograms of the peak locations, the classification accuracy was estimated to be above 93.8 %. As for future work, the accuracy should be improved by decreasing the variations of peak locations. In accordance with the estimated SM area, the developed system achieves 1.5-fold-higher throughput than the conventional prism-type system [15]. Accordingly, the developed system can provide the approach for increasing the throughput of an imaging system for DNA microarray-chip analysis [7] and SM real-time DNA sequencing [8, 9].

Acknowledgments We thank Dr. Osamu Kogi for his helpful advice on sample preparation.

References

1. Sako Y, Minoguchi S, Yanagida T (2000) Single-molecule imaging of EGFR signaling on the surface of living cells. Nat Cell Biol 2:168–172
2. Murakoshi H, Iino R, Kobayashi T, Fujiwara T, Ohshima C, Yoshimura A, Kusumi A (2004) Single-molecule imaging analysis of Ras activation in living cells. Proc Natl Acad Sci U S A 101:7317–7322
3. Yokota H, Saito K, Yanagida T (1998) Single molecule imaging of fluorescently labeled proteins on metal by surface plasmons in aqueous solution. Phys Rev Lett 80:4606–4609
4. Hohng S, Joo C, Ha T (2004) Single-molecule three-color FRET. Biophys J 87:1328–1337
5. Kozuka J, Yokota H, Arai Y, Ishii Y, Yanagida T (2006) Dynamic polymorphism of single actin molecules in the actin filament. Nat Chem Biol 2:83–86
6. Arai Y, Iwane AH, Wazawa T, Yokota H, Ishii Y, Kataoka T, Yanagida T (2006) Dynamic polymorphism of Ras observed by single molecule FRET is the basis for molecular recognition. Biochem Biophys Res Commun 343:809–815
7. Kang SH, Kim Y, Yeung ES (2007) Detection of single-molecule DNA hybridization by using dual-color total internal reflection fluorescence microscopy. Anal Bioanal Chem 387:2663–2671
8. Eid J et al (2009) Real-time DNA sequencing from single polymerase molecules. Science 323:133–138
9. Beechem JM (2010) Single molecule real-time nucleic acid sequencing-by-synthesis using Quantum-dot (Qdot™) nanocrystal and dye-labeled DNA polymerase with FRET-based detection. Adv Genome Biol Technol Conf Book 6
10. Bentley DR et al (2008) Accurate whole human genome sequencing using reversible terminator chemistry. Nature 456:53–59
11. Haga T, Sonehara T, Sakai T, Anazawa T, Fujita T, Takahashi S (2011) Simultaneous four-color imaging of single molecule fluorophores using dichroic mirrors and four charge-coupled devices. Rev Sci Instrum 82:023701
12. Haga T, Takahashi S, Sonehara T, Kumazaki N, Anazawa T (2011) Dual-view imaging system using a wide-range dichroic mirror for simultaneous four-color single-molecule detection. Anal Chem 83:6948–6955
13. Niino Y, Hotta K, Oka K (2009) Simultaneous live cell imaging using dual FRET sensors with a single excitation light. PLoS One 4:e6036
14. Malik Z, Cabib D, Buckward RA, Talmi Y, Garini Y, Lipson SG (1996) Fourier transform multipixel spectroscopy for quantitative cytology. J Microsc 182:133–140
15. Lundquist PM et al (2008) Parallel confocal detection of single molecules in real time. Opt Lett 33:1026–1028
16. Sonehara T, Sakai T, Haga T, Fujita T, Takahashi S (2011) Prism-based spectral imaging of single-molecule fluorescence from gold-nanoparticle/fluorophore complex. J Fluoresc 21:1805–1811
17. Suzuki Y, Tani T, Sutoh K, Kamimura S (2002) Imaging of the fluorescence spectrum of a single fluorescent molecule by prism-based spectroscopy. FEBS Lett 512:235–239
18. Matsuoka H, Kosai Y, Saito M, Takeyama N, Suto H (2002) Single-cell viability assessment with a novel spectro-imaging system. J Biotechnol 94:229–3008
19. Levene MJ, Korlach J, Turner SW, Foquet M, Craighead HG, Webb WW (2003) Zero-mode waveguides for single-molecule analysis at high concentrations. Science 299:682–686
20. ABI PRISM® BigDye Primer Cycle Sequencing ready Reaction Kit Protocol available at http://www3.appliedbiosystems.com/cms/groups/mcb_support/documents/generaldocuments/cms_040937.pdf. Accessed 20 October 2012
21. Tamaru H, Kuwata H, Miyazaki T, Miyano K (2002) Resonant light scattering from individual Ag nanoparticles. Appl Phys Lett 80:1826–1828
22. Bouhelier A, Bachelot R, Lerondel G, Kostcheev S, Royer P, Wiederrecht GP (2005) Surface plasmon characteristics of tunable photoluminescence in single gold nanorods. Phys Rev Lett 95:267405
23. Funatsu T, Harada Y, Tokunaga M, Saito K, Yanagida T (1995) Imaging of single fluorescent molecules and individual ATP turnovers by single myosin molecules in aqueous solution. Nature 374:555–559